# Low-Thermal Noise Input-Filter Design for DC/DC Power Regulators

Ishan Mukherjee\* and Idris A. Gadoura\*\*

\*Department of Mechanical Engineering, Massachusetts Institute of Technology Cambridge, MA 02139-4307 USA (e-mail: ishanm@mit.edu) \*\* Department of Engineering, University of New Brunswick Saint John, NB, Canada E2L 4L5 (e-mail: igadoura@unb.ca)

**Abstract:** In this paper input filters of DC/DC converters used in consumer and industrial electronics are studied and analyzed with an intention of developing a low-noise design. Noise attenuation is carried out by developing noise models for thermal noise in single section input filters of Buck, Boost and Buck-Boost DC/DC converters. The models are applied to a basic buck converter example and simulated to propose attenuation techniques.

Keywords - Power converters, Input Filter Design, Thermal Noise Modeling.

#### 1. INTRODUCTION

Input filters play a major role in conditioning the source power supply to match the load power requirements in nearly all power converter systems. Consequently the requirement of these input filters to be optimally damped has been well appreciated within the power electronics field [1-9]. The importance of input filters design was understood in the early 1970's even before the proper tools to analyze power converters were developed [7], this was exemplified by Middlebrook's benchmark studies [3],[7] dealing with the direct duty-ratio-controlled converters operating continuous inductor current mode. Since then, almost all authors have used similar methodologies when analyzing and designing input filters. Regardless of their circuit topology and control scheme, it is well known that the addition of an input filter to a power converter can adversely affect the converters performance, even to the point of causing instability in the power system. The input filter serves, in general, to isolate the line voltage transients such that the converters performance will not be degraded, and to prevent the power line from being disturbed by the switching current drawn from the input filter output, but it has been researched [8], [9], that, in doing so, the dynamics of the converter is severely altered. Several studies [8] and [9] have been carried out to analyze and negate these unwanted input filer interactions. Furthermore systematic methodologies have been developed to optimally design input filters for power converters. These methodologies state that the stability of the system is ensured, if the amplitude of the output impedance is always less than the amplitude of the input impedance of the converters. Additional criteria have been presented to ensure that the output performance of the converter is not affected. The basic design criteria are extracted from the canonical circuit models developed by Middlebrook and Cuk [7]. In all of these methodologies input filters have been designed to compensate for efficiency losses attributed to input filter

interactions with the dynamics of the converters and specific power losses. These models have no doubt been refined to be highly efficient designs, but it leaves a scope to incorporate the efficiency losses attributed to noise sources both inside the filter-converter system and outside it. In practical applications of power converters, such as the ones in consumer electronics applications, power converters are just one of many components of very large electrical and electronic systems. Being a part of such a system the filter and the converter module is exposed to wide range of noise sources. These noise sources are chiefly in the form of Electromagnetic Interference (EMI), Thermal Noise and in lesser magnitude white noise and 1/f noise sources caused due to inefficient switching. Existing input filters are designed and adequately damped to attenuate the EMI in the converter system under the condition that the Middlebrook criteria are met. In this study we have taken the concept of incorporating noise sources in the filter-converter system to factor in the noise caused by both active and passive modules. A thermal noise model [10] has been developed to generate the power spectral density (PSD) of thermal noise in the passive circuit of an input filter. Using network analysis techniques the filter circuits are reduced to their Thevinin and Norton equivalent forms; this process gives a designer the flexibility of representing the filter impedance as a single impedance block and also provides the design to incorporate exterior noise sources by including their equivalent impedances in the single impedance block of the reduced circuit. The power spectral density of noise is plotted against frequency; the frequency range in the vicinity of the resonant frequency is iteratively studied by varying circuit configurations to generate specific circuit configurations which produce minimal noise without affecting the damping and stability criteria. The analysis is carried out by studying optimally damped single section input filter circuits designed in literatures such as [9] and [11] by manipulating the circuit specifications to develop a low-noise design.

#### 2. THERMAL NOISE MODEL

Thermal noise is associated with the random movement of electrons, due to the electrons thermal energy. As a consequence of such electron movement, there is a net movement of charge, during any interval of time, through an elemental section of a resistive material. Such a net movement of charge is consistent with a current flow, and as the elemental section has a defined resistance, the current flow generates an elemental voltage. The sum of the elemental voltages, each of which has a random magnitude, is a random time varying voltage. Statistical arguments based on the equipartition theorem, by Nyquist in 1928, can be used to show the power spectral density (PSD) of the random process [10]. It can be reasoned that the magnitude of thermal noise is minute and can be ignored, but it is our argument that attenuating thermal noise depends on scalability i.e. the capacity and the efficiency of the power converter being used. In applications such as inverters in DC power transmission where the power converters of about 1000 Megawatts are required, thermal noise significantly reduces efficiency. On the other hand in precise microelectronic systems where power converters are required to maintain complete efficiency over a long period of time, thermal noise attenuation is required to factor in efficiency losses attributed to normal wear and tear of the converter components in the course of continuous operation.

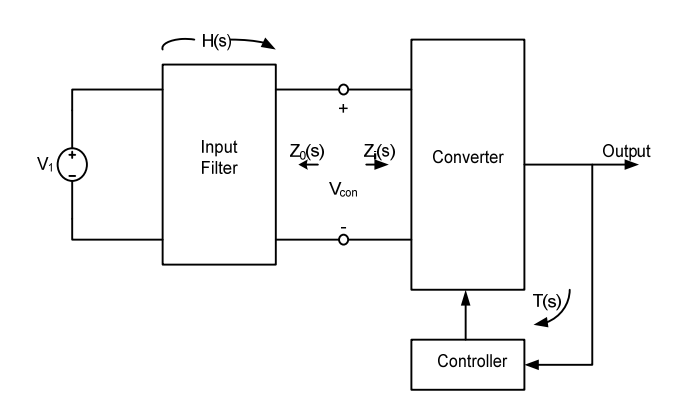


Fig.1. Input Filter- Converter System

# 2.1. Formulation

Irrespective of the type of controller most of the input filters used in practical applications, as shown in Fig. 1, are passive networks with circuits comprised of varying configurations of passive elements such as resistors, transformers, capacitors and inductors. The passive nature of input filter designs has been used to develop a noise model which models the power spectral density (PSD) of the noise as a function of frequency,  $G_v(f)$ .

As shown in Figure 2(a), the input filter module is converted to its Thevinin equivalent, Fig. 2(b), with the voltage source  $V_1$  converted to its Thevinin equivalent  $V_{eq}$ , and the filter impedance converted to a single impedance module with value  $Z_{eq}$ . As explained in [10] this Thevinin equivalent circuit can be used to model the noise in the filter circuit,

producing the power spectral density of noise, measured across the terminal of a passive network, which is a generalization of Nyquist theorem [10].  $G_v(f)$  is defined by:

$$G_V(f) = 2kT \operatorname{Re} \left[ Z_{in}(f) \right] = 2kT R_{in}(f) \quad V^2 / \operatorname{Hz}$$
(1)

where,  $Z_{in}$  = the input impedance at the same two terminals.

$$Z_{in}(f) = Z_{in}(j2\pi f) = R_{in}(j2\pi f) + X_{in}(j2\pi f)$$
(2)

where,  $X_{in}(j2\pi f)$  is the imaginary part and  $R_{in}(j2\pi f)$  is the real part as a result

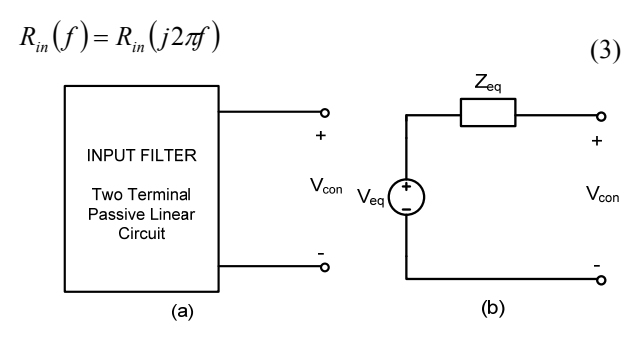


Fig. 2. The vinin equivalent circuit (b) of input filter (a)

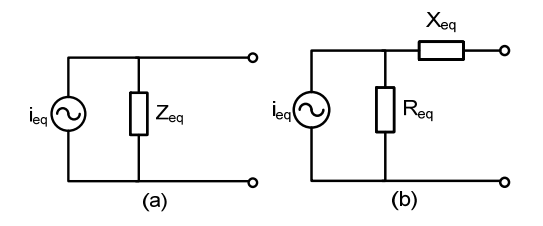


Fig. 3. Norton equivalent circuit models

The proof of equation (1) uses an argument based on conservation of energy as opposed to direct circuit analysis [10]. Similarly power spectral density of the equivalent current sources  $i_{eq}$  in the equivalent models shown in Figures 3(a) and 3(b) is given by equations (4) and (5) respectively

$$Geq(f) = \frac{2kTR_{in}(f)}{|Z_{in}(f)|^{2}} \quad A^{2}/Hz$$

$$G_{eq}(f) = \frac{2kT}{R_{in}(f)} \quad A^{2}/Hz$$

$$\downarrow \qquad \qquad \downarrow \qquad \qquad \downarrow$$

Fig. 4. R– $C_d$  Parallel Damping

#### 2.2. Application

The noise model developed can is implemented on a  $R-C_d$ Parallel Damped input filter which is one of them most widely used single-section damped input filter for DC/DC power converters (Buck, Boost, and Buck-Boost). Figure 4 shows a damped filter made with a resistor R in series with a capacitor  $C_d$ , all connected in parallel with the filter's capacitor C. The purpose of resistor R is to reduce the output peak impedance of the filter at the cutoff frequency. The capacitor  $C_d$  blocks the dc component of the input voltage, and avoids the power dissipation on R. The capacitor  $C_d$ should have lower impedance than R at the resonant frequency, and also be of a larger value than the filter capacitor, to not affect the cutoff point of the main *R*–*L* filter. The output impedance of the filter is the equivalent impedance of the three block impedances  $Z_1$ ,  $Z_2$  and  $Z_3$  in parallel, where

$$Z_1 = R \parallel (1/sC_d), Z_2 = 1/sC \text{ and } Z_3 = sL$$

We have by Thevinin equivalent theorem. The calculation of  $G(f) = 2kT \operatorname{Re}[Z_{eq}(2\pi f)]$  can be summarized by equations (6)-(9).

# 3. SIMULATION ANALYSIS OF R- $C_d$ PARALLEL DAMPED INPUT FILTER

Analysis has been carried out on a R– $C_d$  parallel damped single section input filter as given in the literature [9]. Individual specifications were varied while maintaining the remaining configuration constant. In the numerous stages the effect of variation in the values of  $R_D$ ,  $R_{LF}$ ,  $R_{CF}$  and  $C_D$  was analyzed. The filer circuit as shown in Fig. 4 comprises of a damping module with resistor  $R_D$  in series with a capacitor  $C_D$ . It has been argued that the resistance  $R_D$  includes both the resistance of the capacitor  $R_{CD}$  and the resistance of the damping module  $R_{damping}$ . The purpose of resistor  $R_D$  is to reduce the output peak impedance of the filter at the cutoff frequency. The capacitor  $C_D$  blocks the dc component of the input voltage, and avoids the power dissipation on  $R_D$ . The output impedance of the filter can be calculated from the

equivalent impedance of the three block impedances  $Z_1$ ,  $Z_2$  and  $Z_3$ , where

$$Z_1 = R_{LF} + sL_F (1/sC_d), Z_2 = R_{CF} + 1/sC_F$$
  
and  $Z_3 = R_D + 1/sC_D$ 

Also the Thevinin equivalent circuit is:

$$V_{eq} = \frac{Z_2 \parallel Z_3}{Z_2 \parallel Z_3 + Z_1} V_1$$

$$Z_{eq} = \frac{1}{\frac{1}{Z_1} + \frac{1}{Z_2} + \frac{1}{Z_3}} = \frac{N(s)}{D(s)}$$
(10)

For simulating the power spectral density of noise  $G_v(f)$  of the input filter circuit the following specifications were used [9].

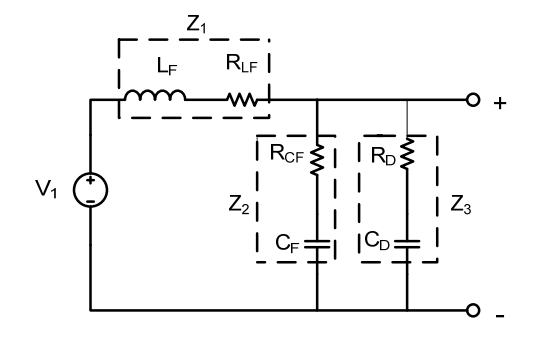


Fig. 5.  $R-C_d$  parallel damped single section input filter

$$L_F = 16 \,\mu\text{H}, \quad C_F = 100 \,\mu\text{F}$$
 
$$R_{LF} = 0.162 \,\Omega, \quad R_{CF} = 5 \,\text{m}\Omega$$

To study the variance of noise caused by variations in damping conditions three sets of damping values were taken,

$$C_D = 100 \,\mu\text{F}, \quad 200 \,\mu\text{F}, \quad 1000 \,\mu\text{F}$$
  
 $R_D = 0.58 \,\Omega, \quad 0.37 \,\Omega, \quad 0.15 \,\Omega$ 

$$V_{eq} = \frac{\frac{Z_1 Z_2}{Z_1 + Z_2}}{\frac{Z_1 Z_2}{Z_1 + Z_2} + Z_3} V_1 = \frac{1 + (RC_b)s}{1 + (RC_b)s + (L(C + C_b))s^2 + (RLCC_b)s^3} V_1$$
(6)

$$Z_{eq} = \frac{1}{\frac{1}{Z_1} + \frac{1}{Z_2} + \frac{1}{Z_3}} = \frac{(L)s + (RLC_b)s^2}{1 + (RC_b)s + (L(C + C_b))s^2 + (RLCC_b)s^3} = \frac{N(s)}{D(s)}$$
(7)

$$\operatorname{Re}\left[Z_{eq}(j2\pi f)\right] = \operatorname{Re}\left[\frac{N(j2\pi f)D(-j2\pi f)}{|D(j2\pi f)|^2}\right]$$
(8)

$$= \frac{\left(8\pi^{2}RLC_{b}\right)f^{2} - \left(16\pi^{4}RL^{2}L_{b}(2C + C_{b})\right)f^{4}}{2 - \left(8\pi^{2}L(C + C_{b})\right)f^{2} - \left(16\pi^{3}RLCC_{b}\right)f^{3} + \left(16\pi^{4}L^{2}(C + C_{b})^{2}\right)f^{4} + \left(8\pi^{3}RLCC_{b}\right)^{2}f^{6}}$$

$$G(f) = \frac{2kT\left[\left(8\pi^{2}RLC_{b}\right)f^{2} - \left(16\pi^{4}RL^{2}L_{b}(2C + C_{b})\right)f^{4}\right]}{2 - \left(8\pi^{2}L(C + C_{b})\right)f^{2} - \left(16\pi^{3}RLCC_{b}\right)f^{3} + \left(16\pi^{4}L^{2}(C + C_{b})^{2}\right)f^{4} + \left(8\pi^{3}RLCC_{b}\right)^{2}f^{6}}$$

$$(9)$$

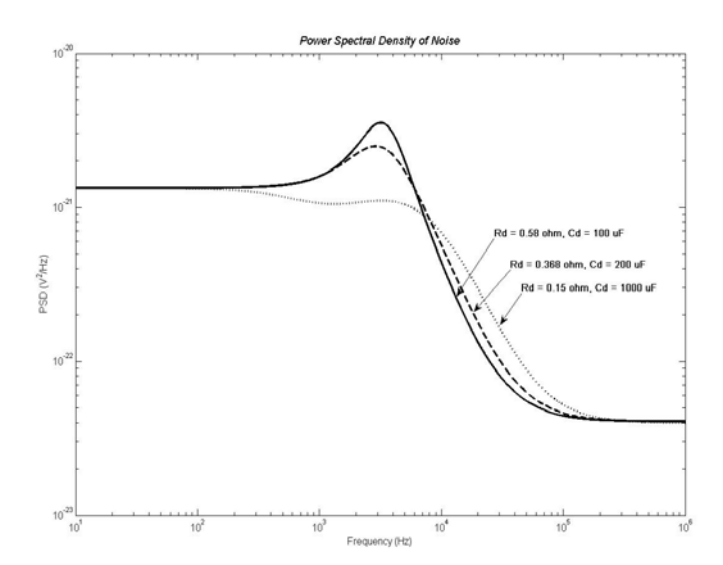


Fig. 6. Power spectral density (PSD)  $G_{\nu}(f)$  function of noise in the  $R-C_d$  Parallel Damping

Fig. 6. shows the Power Spectral density of Noise  $G_{\nu}(f)$  for the three sets of damping values. The second condition  $C_D$ =  $200\mu F$  and  $R_D = 0.37\Omega$  provides the most ideal damping specification according to the literature [9]. It can be observed from the graph that in the lower frequency range varying up to 0.7 kHz and in the high frequency range after 100kHz the  $G_{\nu}(f)$  values for al three configurations are nearly equal with the overlapping asymptotes. The frequency range around the resonant frequency poses the most interesting area for analysis. It can be observed that the noise for the third case i.e.  $C_D$ = 1000 $\mu$ F and  $R_D$ = 0.15 $\Omega$  is the least in this region; this can be attributed to the small resistance value and very large capacitance. On the other hand the other two configurations illustrate that the configuration of  $C_D$ = 200 $\mu$ F and  $R_D$ = 0.37 $\Omega$ , which provides the most ideal damping it also produces lesser magnitude of noise that the first configuration  $C_D$ = 100 $\mu$ F and  $R_D$ = 0.58 $\Omega$ . In practical cases the most efficient method of noise attenuation would be to achieve minimal noise by changing the resistance values existing in the filter circuit as alteration of inductors and conductors in existing circuits is both cumbersome and inefficient. Therefore the experiments mainly deal with the analysis of  $G_{\nu}(f)$  plots of noise with respect to the three resistance modules in the filter circuit with exception of the damping capacitor as the damping circuit is placed externally in many cases or more easily accessible than the filter inductance and capacitance branches.

#### A. Varying resistance R<sub>D</sub>

In this particular analysis the damping resistance value  $R_D$  has been varied with the remaining circuit configurations being the same as earlier. In the first stage illustrated by Fig. 7 the simulation is carried out by varying the value of  $R_D$  over a small range on both sides of the optimally damped resistance value of  $R_D$ = 0.365 $\Omega$ , with  $R_D$ = 0.265 $\Omega$  and 0.465 $\Omega$ , being the other two values. This close range simulation is carried out to illustrate how the general P.S.D. of Noise varies with variation in  $R_D$  values. It can be clearly seen that in the low frequency range (<1 kHz) and high

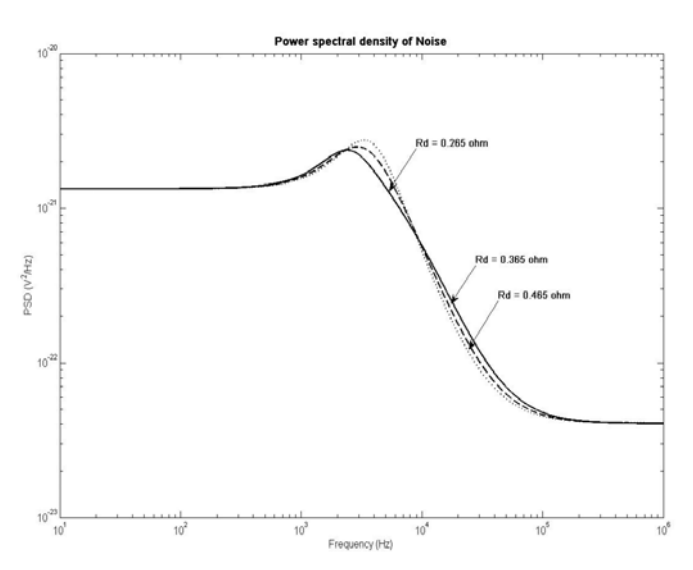


Fig. 7. Power spectral density (PSD)  $G_v(f)$  of noise with close range variation in  $R_D$ 

frequency range (>100 kHz) the asymptotes coincide showing very little variance in the magnitude of noise. However in the region near the resonant frequency (1 kHz-100 kHz) the magnitude of noise increases with the increase in the value of resistance and after the resonant frequency the curves basically follow each other to later coincide in the high frequency range. In the second stage illustrated by the Fig. 8. the analysis is carried over a wider range of  $R_D$  with  $R_D = 0.265\Omega$ ,  $1.365\Omega$  and  $7.465\Omega$ . This is carried out so to study the magnitude in of the change in noise with variation in  $R_D$ . It can be seen that as resistance increases the peak of the  $G_{\nu}(f)$  asymptote also increases signifying increase in the magnitude of noise. It must be noted that it was observed that on increasing the resistance value beyond  $3\Omega$  the increase in the peak value started decreasing and eventually stagnated in around  $9\Omega$ , this can be attributed to the capacitor placed in series with  $R_D$  which limits the amount of current flowing through it. Irrespective of the resistance value the magnitude of noise remains same in the low and high frequency ranges with the asymptotes coinciding. The above mentioned variations occur in the resonant frequency range.

Table 1. The variations in  $R_D$ 

$R_D$	Peak Value	Frequency
7.465Ω	$7.278 \times 10^{-21} \text{V}^2 / \text{Hz}$	3.801 kHz
1.365Ω	4.753×10 <sup>-21</sup> V <sup>2</sup> /Hz	3.817 kHz
0.265Ω	$2.449 \times 10^{-21} \text{V}^2 / \text{Hz}$	2.286 kHz

These peak values show how the magnitude of noise increase with the increase in resistance value before and at the resonant frequency and after peaking the asymptotes follow each other to coincide near the 100 kHz frequency range. The resistance  $R_D$  provides flexibility because of its positioning and significance.

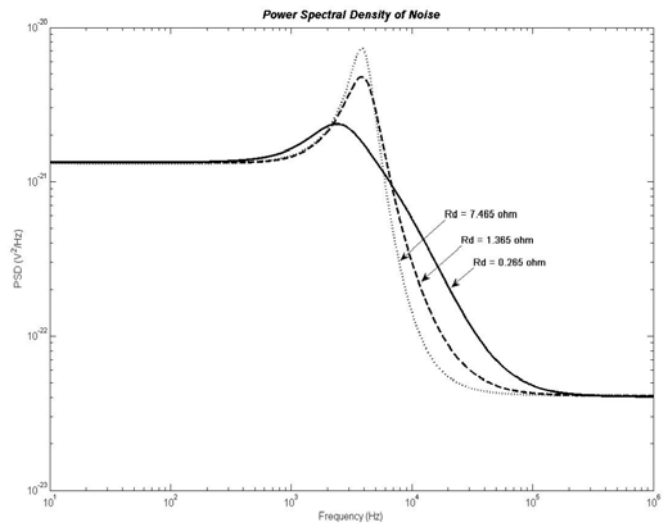


Fig. 8. PSD  $G_{\nu}(f)$  of noise with wide range variation in  $R_D$ 

The internal resistance of the capacitor  $C_D$  can be incorporated in to  $R_D$  and on requirement can be comparatively easily altered. With the repeated use of a power converter the passive components in the input filter gradually become less efficient, thus increasing noise in the system. This form of analysis gives a designer the tool to replace a particular specification to attenuate noise without violating the damping and stability criteria.

#### B. Varying capacitance $C_D$

The second experimental analysis is carried out by varying the value of the damping capacitance  $C_D$  keeping all other specification constant. The capacitance value was varied through wide range with  $C_D$ = 2000 $\mu$ F, 200 $\mu$ F and 20 $\mu$ F. Large values of capacitance were not considered as it would not satisfy the stability criteria of the input filter design. As illustrated by Fig. 9. The magnitude of nose does not vary much with the variation in the magnitude of  $C_D$ . At high capacitance values the  $C_D$  offers high impedance path for current thus producing constant noise. At low capacitance values the noise at resonant frequency is slightly larger than at higher values as after complete charging it provides a low impedance path for filter current. This can be proven by the peak values of the respective graphs. The peak value of  $G_{\nu}(f)$ when  $C_D = 20 \mu \text{F}$  is  $6.23 \times 10^{-21} \text{ V}^2/\text{Hz}$  where as the peak values for the other two configurations are around  $4.94 \times 10^{-21} \text{ V}^2/\text{Hz}$ around the resonant frequency region. Therefore it can be concluded that noise contributed by the damping capacitance  $C_D$  is constant and relatively uniform over a wide range of capacitance values, providing little scope for noise attenuation.

## C. Varying resistance $R_{LF}$

In this experiment the resistance  $R_{LF}$ , which is placed in series with inductor  $L_D$  is varied and analyzed. In the first stage (Fig. 10.) the resistance  $R_{LF}$  is varied over a short—with  $R_{LF} = 0.1\Omega$ ,  $0.162\Omega$  and  $0.2\Omega$ . In the low frequency range (<1 kHz) the noise asymptotes increase with gradual increase in  $R_{LF}$  values, thus indicating greater presence of noise for larger  $R_{LF}$  values. In the resonant frequency region the P.S.D. asymptotes peak at the resonant frequency and the gradually

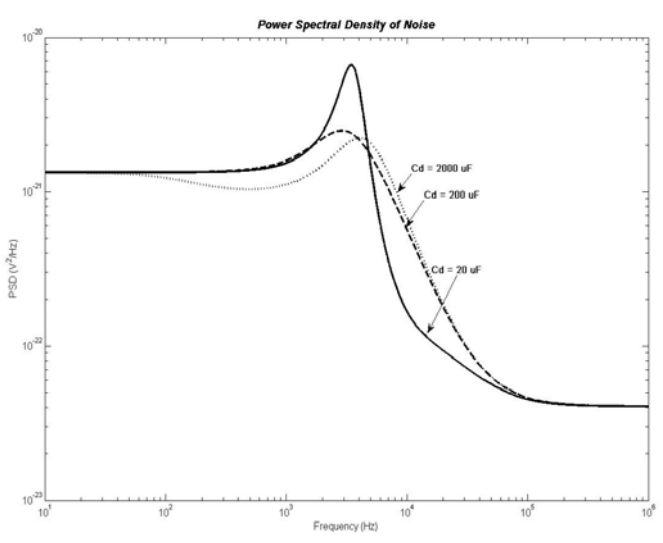


Fig. 9. PSD  $G_{\nu}(f)$  of noise with small range variation in  $R_D$ 

decrease to coincide into equal asymptotes. It is clearly observed that the peak values for higher  $R_{LF}$  values produce smaller peaks than by lower  $R_{LF}$  values. After peaking and in the high frequency region (>100 kHz) the magnitude of noise decrease and becomes constant for all values of  $R_{LF}$ . In the second stage (Fig. 11.), the resistance  $R_{LF}$  is varied over a wider range of values where  $R_{LF}$ = 0.5 $\Omega$ , 1 $\Omega$  and 5 $\Omega$ . The trends observed in the previous stage are followed here but to a larger extent. In the low frequency range the noose produced by higher  $R_{LF}$  values are significantly and uniformly higher than for smaller  $R_{LF}$  values. As the magnitude of  $R_{LF}$  is increased the magnitude of noise in the low frequency range also increases to a point after which the resonant peaking is of a lesser magnitude than the low frequency noise. In the resonant frequency region the peaking magnitude decreases after which the asymptotes coincide in the high frequency region. Thus it is inferred that the resistance  $R_{LF}$  placed in the inductor branch produces significant noise in the low frequency region which increases with the increase in resistance value and this leads to a peaking in the resonant frequency region whose magnitude decreases with increase in  $R_{LF}$  magnitude and the noise gradually decrease attaining similar value for all relevant values of  $R_{LF}$ . This makes evident the significant role of  $R_{LF}$ in low frequency regions which can be attenuated by decreasing the magnitude of resistance; this would also decrease the noise peaking in the resonant frequency region.

#### D. Varying resistance $R_{CF}$

Fig. 12 illustrates the power spectral density of noise in filer circuit on the variation of capacitance resistance  $R_{CF}$ . The scope of this experiment is limited as  $R_{CF}$  constitutes the resistance offered by the capacitor, which is constant for all practical purposes and only varies after the charging of the capacitor, furthermore implementing any alterations in the  $R_{CF}$  resistance would be highly cumbersome. The magnitude of resistance  $R_{CF}$  is varied over a range of  $R_{CF} = 0.5 \text{m}\Omega$ ,  $5 \text{m}\Omega$  and  $50 \text{m}\Omega$ . It can be observed that in the low frequency range (<1 kHz) the noise remains equal and constant, and then it gradually peaks at the resonant frequency range without any variation with frequency.

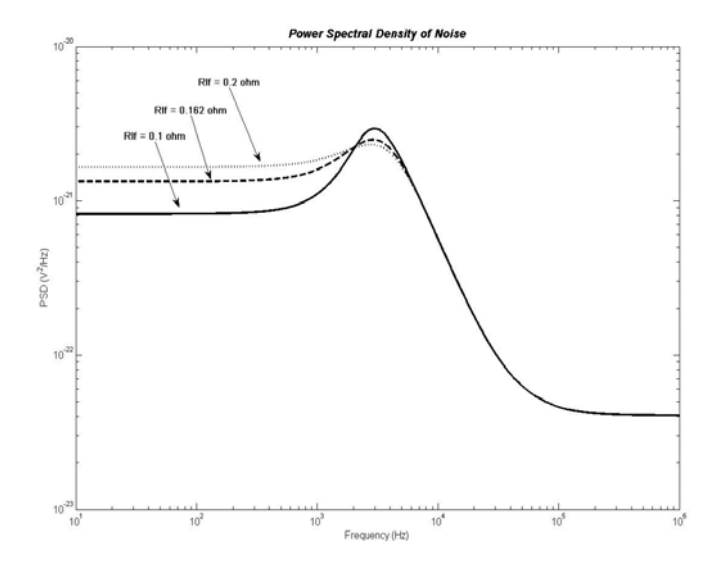


Fig. 10. PSD  $G_{\nu}(f)$  of noise with variation in  $R_{LF}$ 

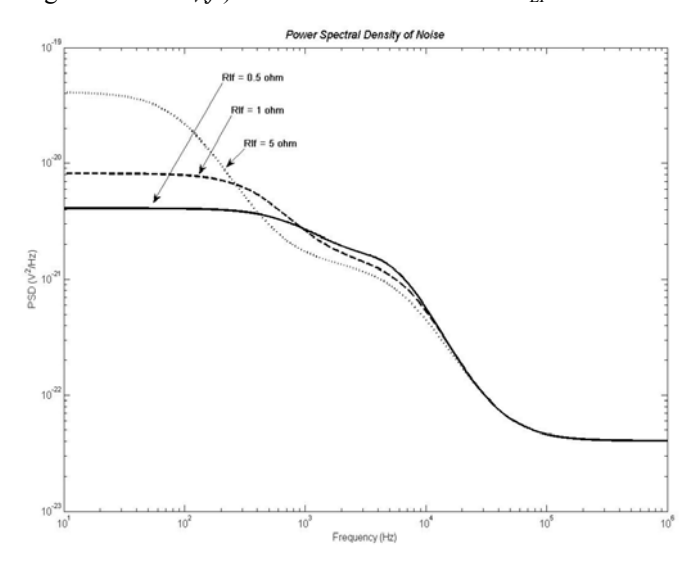


Fig. 11. PSD  $G_{\nu}(f)$  of noise with variation in  $R_{LF}$ 

### 3. CONCLUSION

The passive nature of input filter designs as been used to develop a noise model which models the power spectral density (PSD) of the noise as a function of frequency G<sub>n</sub>(f). This versatile model allows modeling of any form of passive input filter circuit by representing the total impedance in the filter circuit in the form a single equivalent impedance module along with an equivalent voltage supply, this can be done by using network analysis tools. Then noise model is implemented in a widely used  $R-C_d$  parallel damped input filter, subsequent analysis showed that the resistances  $R_D$  and  $R_{LF}$  provide the best viability for noise attenuation. The damping resistance  $R_D$  can be decreased to account for the future increase in resistance due to operational losses; at the same time satisfying damping and stability criteria. The inductor resistance  $R_{LF}$  can be modified to account for the inductor losses caused due to the individual inductor degradation and also inductor losses caused by electrical and electronic components of other systems in the vicinity. A calculated increase in  $R_{LF}$  value would increase the noise in the low frequency bandwidth but would decreases the noise

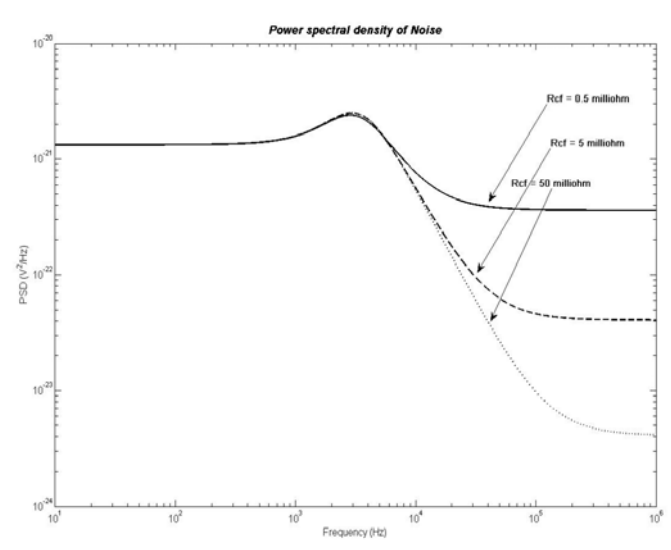


Fig. 12. PSD  $G_{\nu}(f)$  of noise with variation in  $R_{CF}$ 

peaks thus reducing efficiency losses. Thus although the resistance  $R_{LF}$  represents the resistance offered by the inductor  $L_F$ , it offers flexibility to be altered according to requirements to attenuate noise. Therefore, in this paper a simple, comprehensive and highly flexible model to represent noise in an input filter for a DC/DC converter, explaining the procedures involved in the simulation and analysis of noise.

#### REFERENCES

- Fischer W. and A. Lindemann, "Circuit simulation in a research oriented education of power electronics," COMPEL 2008, 17-20 Aug. pp. 1-5.
- 2 Erickson Robert W. and Maksimovic D., "Fundamentals of Power Electronics," 2<sup>nd</sup> ed.n, Kluwer Academic Publishers. 2001. pp. 377-398.
- 3 Middlebrook R.D, "Input Filter Considerations in Design and Application of Switching Regulator," IAS '76. pp. 366-382.
- 4 Lee F.C. and Y. Yu, "Input-Filter Design for Switching Regulator," IEEE Trans. on Aerospace and Electronic Systems. Vol. AES-15. No.5 Sep.1979. pp .627-634.
- 5 Erichand S.Y. and W.M. Polivka, "Input Filter Design for Current-Programmed Regulator," Proc. of the IEEE APEC '90. pp. 781-791.
- 6 Wu T-F., K. Siri, and C. Q. Lee, "A systematic method in designing line filters for switching regulators," in Proc. IEEE APEC'92. 1992. pp. 179-18.
- Middlebrook R. D. and S.Cuk`, "A general unified approach to modeling switching-converter power stages," Int. J. Electron. Vol. 42 .1979., No. 6, pp. 521–550.
- 8 Dongsoo Kim; Byungcho Choi; Donggyu Lee and Jian Sun, "Analysis of input filter interactions in switching power converters", APEC 2005. Vol. 1, pp. 191-198.
- 9 Suntio T., I. Gadoura, and K. Zenger, Input filter interactions in peak-current-mode-controlled buck converter operating in CICM," IEEE Trans. Industrial Electron. Vol. 49., Feb. 2002. pp. 76-86.
- 10 Howard Roy M., "Principles of random signal analysis and low noise design-the power spectral density and its applications," John Wiley & Sons, Inc. 2002. pp 287-291.
- 11 Erickson Robert W., "Optimal Single Resistor Damping of Input Filters," Colorado Power Electronics Center, University of Colorado, Boulder, Colorado 80309-0425.